Dinuclear $Cu^{II}M^{II}$ (M = Co, Ni, Cu or Zn) and $Cu^{II}Cu^{I}$ Complexes of a Phenol-based Dinucleating Macrocycle with Dissimilar N_2O_2 and N_2O_2S Sites†

Shin-ichiro Ohtsuka,[a] Masahito Kodera,[b] Ken-ichiro Motoda,[a] Masaaki Ohba[a] and Hisashi Ōkawa*[,a]

[a] *Department of Chemistry, Faculty of Science, Kyushu University, Hakozaki 6-10-1, Higashiku, Fukuoka 812, Japan*

[b] *Department of Molecular Science and Technology, Faculty of Engineering, Doshisha University, Tanabe-cho, Kyoto 610-03, Japan*

A dinucleating macrocycle H_2L with two 2,6-bis(iminomethyl)-4-methylphenolate entities combined through two lateral chains, CH_2CH_2 and $CH_2CH_2SCH_2CH_2$, at the imino nitrogens has been obtained as a mononuclear copper(II) complex $[Cu(H_2L)][ClO_4]_2$. It reacted with a second metal ion under alkaline conditions to form dinuclear complexes $[Cu^{II}M^{II}L(NCS)_2]\cdot H_2O$ (M = Co, Ni or Zn), $[Cu^{II}Cu^{II}L][ClO_4]_2$ and $[Cu^{II}Cu^{I}L]ClO_4$. The crystal structure of the dimethylformamide adduct, $[CuZnL(NCS)_2]\cdot$dmf, reveals the discrete CuZn dinuclear structure bridged by the two phenolic oxygens of $(L)^{2-}$. The Cu^{II} resides at the site with the CH_2CH_2 lateral chain and assumes a square-pyramidal geometry together with an isothiocyanato nitrogen at the apex. The Zn^{II} is at the site with the $CH_2CH_2SCH_2CH_2$ chain and assumes a similar square-pyramidal geometry with an isothiocyanato nitrogen at the apex. The sulfur on the lateral chain is not co-ordinated but disposed to the Zn^{II} with the Zn · · · S separation of 3.48 Å. An antiferromagnetic spin exchange operates in the $Cu^{II}M^{II}$ (M = Co, Ni or Cu) complexes (J = −32 cm^{-1} for M = Co, −90 cm^{-1} for M = Ni and −440 cm^{-1} for M = Cu based on $H = -2JS_1S_2$). In cyclic voltammograms of $[Cu^{II}Cu^{II}L][ClO_4]_2$ and $[Cu^{II}Cu^{I}L]ClO_4$ the copper ion at the site with the $CH_2CH_2SCH_2CH_2$ lateral chain shows a reversible Cu^{II}–Cu^{I} redox couple at ≈ +0.08 V (*vs.* saturated calomel electrode).

Recently there has been increasing interest in heterodinuclear complexes with the aim of designing new functional systems for incorporating and activating simple molecules[1–3] and to explore the mutual effects of two metal ions upon the physicochemical properties of such complexes.[4–6] The use of macrocyclic ligands (macrocycles hereafter) for this purpose is of great advantage because heterodinuclear cores can be stabilized by the macrocyclic effect.[7] Further, the core structure and physicochemical properties of heterodinuclear complexes can be modulated by changing the macrocycles.[8]

In previous studies[9,10] we have reported a phenol-based dinucleating macrocycle H_2L' possessing two different metal-binding sites with N_2O_2 and N_3O_2 donor sets, sharing the two phenolic oxygens. It forms a series of dinuclear $Cu^{II}M^{II}$ and $Ni^{II}M^{II}$ (M = Mn, Fe, Co, Ni, Cu or Zn) complexes with the Cu^{II} or Ni^{II} at the N_2O_2 site and the M^{II} at the N_3O_2 site. The metal(II) ion at the N_3O_2 site assumes a highly distorted geometry owing to the co-ordination of the secondary nitrogen on the lateral chain and because of this distortion the metal is stabilized towards oxidation to M^{III}. For example, the oxidation of Mn^{II} or Co^{II} at the N_3O_2 site is more difficult than that of Cu^{II} or Ni^{II} at the N_2O_2 site.

One of our objects with H_2L' and related macrocycles is to provide functional heterodinuclear cores. In this context our next target may be the $M^{II}Cu^{I}$ (M = Mn, Fe or Co) complexes with M^{II} at the planar N_2O_2 site and Cu^{I} at the distorted N_3O_2 site: the salen [H_2salen = *N*,*N*′-bis(salicylidene)ethane-1,2-diamine] complexes of Mn^{II}[11] and Co^{II},[12] having a similar co-ordination to the metal at the N_2O_2 site, are known to take up dioxygen and that of Fe^{II}[13] is very sensitive towards dioxygen. Our preliminary study however, showed that the N_3O_2 site of H_2L' has a relatively low affinity for Cu^{I}, as evidenced by the deposition of metallic copper in attempts to prepare the $Fe^{II}Cu^{I}$ complex. Since it is generally known that sulfur has a high affinity for Cu^{I}, we aimed in this study to prepare an analogous macrocycle (H_2L) with thioether sulfur instead of the secondary amino nitrogen. This paper describes the template synthesis of a mononuclear copper(II) complex of H_2L $[Cu(H_2L)][ClO_4]_2$, and the use of the complex as the precursor for heterodinuclear $Cu^{II}M^{II}$ (M = Co, Ni, Cu or Zn) complexes and a mixed-valence $Cu^{II}Cu^{I}$ complex.

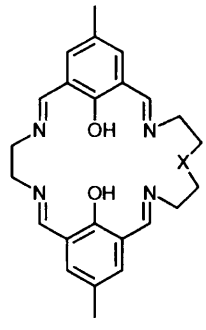

X
H_2L' NH
H_2L S

† *Supplementary data available* (No. SUP 57096, 8 pp.): magnetic susceptibility curves, ESR spectrum and cyclic voltammogram. See Instructions for Authors, *J. Chem. Soc., Dalton Trans.*, 1995, Issue 1, pp. xxv–xxx.

Non-SI unit employed: $\mu_B \approx 9.27 \times 10^{-24}$ J T^{-1}.

Experimental

Measurements.—Elemental analyses of C, H and N were obtained from the Service Centre of Elemental Analysis at Kyushu University. Analyses of metals were made on a Shimadzu AA-680 atomic absorption/flame emission spectrophotometer. Infrared spectra were recorded on a JASCO IR-810 spectrophotometer using KBr discs or Nujol mulls, electronic spectra in dimethylformamide (dmf) on a Shimadzu UV-210 spectrophotometer at room temperature. Magnetic susceptibilities were measured on a Faraday balance in the temperature range 80–300 K and on a HOXAN HSM-D SQUID susceptometer in the range 4.2–80 K. The apparatus was calibrated with $[Ni(en)_3][S_2O_3]$[14] (en = ethane-1,2-diamine) and diamagnetic corrections were made using Pascal's constants.[15] Cyclic voltammograms were recorded on an apparatus comprising a Hokuto Denko HA-501 potentiostat and a HB-104 function generator. Measurements were carried out in dmf solutions (*ca.* 1×10^{-3} mol dm^{-3}) containing tetraethylammonium perchlorate as the supporting electrolyte (**CAUTION**: this perchlorate is explosive and should be handled with care). A three-electrode cell equipped with a glassy carbon working electrode, a platinum coil as the auxiliary electrode, and a saturated calomel electrode (SCE) as the reference was used. X-Band ESR spectra were recorded on a JES-FE3X spectrometer.

Materials.—2,6-Diformyl-4-methylphenol was prepared by a modification[16] of the method of Denton and Suschitzky.[17] *N*,*N*′-bis(3-formyl-5-methylsalicylidene)ethane-1,2-diamine was obtained by the literature method.[16] *N*-(*p*-Tolylsulfonyl)aziridine was prepared by a modification of the procedure of Martin and Bulkowski.[18] Other chemicals were of reagent grade and used as supplied.

Preparations.—*3-Thiapentane-1,5-diamine.* *N*-(*p*-Tolylsulfonyl)aziridine (71.0 g, 0.36 mol) and triethylammonium chloride (24.8 g, 0.18 mol) were suspended in anhydrous dmf (300 cm^3). To the suspension was added potassium hydrogensulfide (16.0 g) in an argon atmosphere and the mixture was stirred for 5 h. Liberated triethylamine was removed by distillation and the residue was poured onto ice–water (*ca.* 3000 cm^3). The resulting orange mass was dissolved in dichloromethane (800 cm^3), and the solution was washed with water, dried with anhydrous sodium sulfate, and diffused with hexane to give *N*,*N*′-bis(*p*-tolylsulfonyl)-3-thiapentane-1,5-diamine as orange crystals. Yield: 67.6 g (88%). Selected IR data (KBr disc): 3280, 1595, 1320 and 1155 cm^{-1}. ^1H NMR (*vs.* $SiMe_4$ in $CDCl_3$): δ 7.74 (d, 4 H), 7.31 (d, 4 H), 5.06 (t, 2 H), 3.08 (q, 4 H), 2.55 (t, 4 H) and 2.43 (s, 6 H).

A mixture of *N*,*N*′-bis(*p*-tolylsulfonyl)-3-thiapentane-1,5-diamine (48.9 g, 0.114 mol), phenol (80 g), and an acetic acid solution of hydrogen bromide (40%, 1100 cm^3) was refluxed for 36 h. An acetic acid solution of hydrogen bromide (40%, 600 cm^3) was added and the mixture was refluxed for 36 h. The reaction mixture was concentrated to *ca.* 500 cm^3 and shaken with three portions (900 cm^3) of dichloromethane–water (1 : 1 v/v). The aqueous layers were combined, washed with three portions (100 cm^3) of dichloromethane, and evaporated to dryness. Trituration of the residue with a small amount of anhydrous ethanol gave 3-thiapentane-1,5-diamine dihydrobromide as a pale coloured powder. It was separated, washed with a small amount of anhydrous ethanol, and dried *in vacuo*. Yield 28.8 g (89%). Free 3-thiapentane-1,5-diamine was liberated by treating the salt with sodium ethoxide in ethanol and used for the following synthesis without further purification.

$[Cu(H_2L)][ClO_4]_2$ **1**. An ethanolic solution of 3-thiapentane-1,5-diamine (240 mg, 2 mmol) was added dropwise to a suspension of [*N*,*N*′-bis(3-formyl-5-methylsalicylidene)ethane-1,2-diaminato]copper(II) (830 mg, 2 mmol) and $Pb(ClO_4)_2 \cdot 3H_2O$ (920 mg, 2 mmol) in ethanol, and the mixture was refluxed for 2 h and acidified with perchloric acid to pH ≈ 3 to give a yellowish brown powder. It was dissolved in acetonitrile and the solution was diffused with diethyl ether to give greenish brown crystals. Yield: 940 mg (67%) (Found: C, 41.40; H, 4.05; Cu, 8.90; N, 8.15. Calc. for $C_{24}H_{28}Cl_2CuN_4O_{10}S$: C, 41.25; H, 4.05; Cu, 9.10; N, 8.00%), μ_{eff} at 290 K 1.77 μ_B. Selected IR data (KBr disc): 3250–3100, 1640, 1080 and 620 cm^{-1}. UV/VIS [λ_{max}/nm (ε/dm^3 mol^{-1} cm^{-1})] in dmf: 405 (20 500) and 610 (250).

$[CuCoL(NCS)_2] \cdot H_2O$ **2**. This complex was prepared in an argon atmosphere to avoid oxidation from atmospheric dioxygen. A methanolic solution (20 cm^3) of **1** (140 mg, 0.2 mmol), $Co(ClO_4)_2 \cdot 6H_2O$ (35 mg, 0.2 mmol) and NaNCS (130 mg, 1.6 mmol) was neutralized with triethylamine to pH 7 and the mixture was refluxed for 4 h. The resulting deep green microcrystals were filtered off, washed successively with methanol and diethyl ether, and dried *in vacuo*. Yield: 123 mg (91%) (Found: C, 45.25; H, 3.80; Co, 8.00; Cu, 9.15; N, 12.25. Calc. for $C_{26}H_{28}CoCuN_6O_3S_3$: C, 45.20; H, 4.10; Co, 8.55; Cu, 9.20; N, 12.15%), μ_{eff} per CuCo at 290 K 4.72 μ_B. Molar conductance (Λ_M/S cm^2 mol^{-1}) in dmf: 85. Selected IR data (KBr disc): 2080, 2070, 1640, 1630 and 480 cm^{-1}. UV/VIS data [λ_{max}/nm (ε/dm^3 mol^{-1} cm^{-1})] in dmf: 375 (12 900) and 560 (210).

$[CuNiL(NCS)_2] \cdot H_2O$ **3**. To a suspension of $Ni(ClO_4)_2 \cdot 6H_2O$ (185 mg, 0.5 mmol) and complex **1** (350 mg, 0.5 mmol) in methanol (70 cm^3), triethylamine was added dropwise to adjust the pH to 7. The mixture was refluxed for 1 h and then filtered to separate any insoluble material. The addition of a methanolic solution of NaNCS (810 mg, 10 mmol) to the filtrate resulted in the precipitation of a greenish powder. This was separated, washed successively with methanol and diethyl ether, and dried *in vacuo*. Yield: 273 mg (79%) (Found: C, 45.25; H, 3.85; Cu, 9.15; N, 12.00; Ni, 8.45. Calc. for $C_{26}H_{28}CuN_6NiO_3S_3$: C, 45.20; H, 4.10; Cu, 9.20; N, 12.15; Ni, 8.50%), μ_{eff} per CuNi at 290 K 3.01 μ_B. Molar conductance (Λ_M/S cm^2 mol^{-1}) in dmf: 90. Selected IR data (KBr disc): 2100, 2080, 1650, 1630 and 480 cm^{-1}. UV/VIS data [λ_{max}/nm (ε/dm^3 mol^{-1} cm^{-1})] in dmf: 370 (13 800) and 550 (150).

$[CuZnL(NCS)_2] \cdot H_2O$ **4**. This complex was obtained as deep green microcrystals in a way similar to that of **3**. Yield: 91% (Found: C, 44.75; H, 3.75; Cu, 9.05; N, 12.05; Zn, 9.50. Calc. for $C_{26}H_{28}CuN_6O_3S_3Zn$: C, 44.75; H, 4.05; Cu, 9.10; N, 12.05; Zn, 9.35%), μ_{eff} per Cu at 297 K 1.86 μ_B. Molar conductance (Λ_M/S cm^2 mol^{-1}) in dmf: 75. Selected IR data (KBr disc): 2080, 1640, 1630 and 480 cm^{-1}. UV/VIS data [λ_{max}/nm (ε/dm^3 mol^{-1} cm^{-1})] in dmf: 370 (13 900) and 540 (140).

A portion of complex **4** was dissolved in dmf and the solution was diffused with diethyl ether to form a dmf adduct $[CuZnL(NCS)_2] \cdot$dmf **4′** as dark green prisms suitable for single-crystal structure analysis (Found: C, 46.30; H, 4.50; Cu, 8.45; N, 12.95; Zn, 9.05. Calc. for $C_{29}H_{33}CuN_7O_3S_3Zn$: C, 46.25; H, 4.40; Cu, 8.45; N, 13.05; Zn, 8.70%).

$[Cu_2L][ClO_4]_2$ **5**. A solution of $Cu(ClO_4)_2 \cdot 6H_2O$ (370 mg, 1 mmol) and complex **1** (700 mg, 1 mmol) in acetonitrile (20 cm^3) was neutralized with triethylamine to pH 7, and the mixture was refluxed for 30 min. The resulting reddish solution was concentrated to *ca.* 10 cm^3 and diffused with diethyl ether to give reddish brown crystals. Yield: 530 mg (70%) (Found: C, 38.10; H, 3.50; Cu, 16.50; N, 7.50. Calc. for $C_{24}H_{26}Cl_2Cu_2N_4O_{10}S$: C, 37.90; H, 3.45; Cu, 16.70; N, 7.35%), μ_{eff} per Cu at 290 K 0.67 μ_B. Molar conductance (Λ_M/S cm^2 mol^{-1}) in dmf: 130. Selected IR data (KBr disc): 1640, 1630, 1140, 1100, 1080 and 620 cm^{-1}. UV/VIS data [λ_{max}/nm (ε/dm^3 mol^{-1} cm^{-1})] in dmf: 380 (12 000), 560 (≈200) and 760 (70).

$[Cu_2L]ClO_4$ **6**. A solution of $[Cu(MeCN)_4]ClO_4$ (330 mg, 1 mmol) and complex **1** (700 mg, 1 mmol) in acetonitrile (15 cm^3) was neutralized with triethylamine to pH 7, and the mixture was refluxed for 2 h. The resulting purple microcrystals were separated, washed with diethyl ether, and dried *in vacuo*. Yield: 570 mg (86%) (Found: C, 43.70; H, 4.00; Cu, 18.40; N, 8.50. Calc. for $C_{24}H_{26}ClCu_2N_4O_6S$: C, 43.60; H, 3.95; Cu, 19.20, N,

8.50%), μ_{eff} per Cu_2 at 290 K 1.83 μ_B. Molar conductance (Λ_M/S cm^2 mol^{-1}) in dmf: 60. Selected IR data (KBr disc): 1640, 1630, 1100, 1080 and 620 cm^{-1}. UV/VIS data [λ_{max}/nm (ε/dm^3 mol^{-1} cm^{-1})] in dmf: 385 (14 000) and 550 ($\approx$150).

X-Ray Structural Analysis of [CuZnL(NCS)$_2$]·dmf **4'**.—A crystal with approximate dimensions 0.3 × 0.3 × 0.4 mm sealed in a glass tube was used for the X-ray diffraction study. Intensities and lattice parameters were obtained on a Rigaku AFC/5 automated four-circle diffractometer, using graphite-monochromated Mo-Kα radiation (λ = 0.710 69 Å) at 20 °C. Lattice parameters and their estimated standard deviations were obtained from a least-squares fit to 20 reflections in the range 25 < 2θ < 36°. Pertinent crystallographic parameters are summarized in Table 1. For the intensity data collections, the ω–2θ scan mode was used at a scan rate of 2° min^{-1}. The octant measured was $+h$, $+k$, $\pm l$. Two standard reflections were monitored every 150 measurements and showed no systematic decrease in intensity. The intensity data were corrected for Lorentz and polarization factors, but not for absorption. 3996 Independent reflections with $|F_o| > 3\sigma(|F_o|)$ in the range 2.5 < 2θ < 48° were assumed to be observed.

The structure was solved by the direct method and refined by block-diagonal least-squares calculations. Reliability factors were defined as $R = \Sigma||F_o| - |F_c||/\Sigma|F_o|$ and $R' = \{\Sigma[w(|F_o| - |F_c|)^2]/\Sigma[w|F_o|^2]\}^{\frac{1}{2}}$ with weights $w = [\sigma(F_o)]^{-1}$. Atomic scattering factors were taken from ref. 19. Hydrogen atoms bound to carbons were introduced in calculated positions. These hydrogen atoms were included in the structure-factor calculation but not refined. Computations were made as described previously.[9] The final R and R' values were 0.0799 and 0.0778, respectively. The final atomic coordinates are given in Table 2.

Additional material available from the Cambridge Crystallographic Data Centre comprises H-atom coordinates, thermal parameters and remaining bond lengths and angles.

Table 1 Crystal data for [CuZnL(NCS)$_2$]·dmf **4'**

Formula	$C_{29}H_{33}CuN_7O_3S_3Zn$
Colour	Dark green
M	752.74
Crystal dimensions/mm	0.25 × 0.3 × 0.4
Crystal system	Monoclinic
Space group	$P2_1/n$
a/Å	14.990(6)
b/Å	18.640(4)
c/Å	12.016(2)
β/°	102.55(2)
U/Å^3	3277(2)
Z	4
D_c/g cm^{-3}	1.526
D_m/g cm^{-3}	1.520
μ(Mo-Kα)/cm^{-1}	16.25
No. of reflections	3996
R^a	0.0799
R'^b	0.0778

^{a} $R = \Sigma||F_o| - |F_c||/\Sigma|F_o|$. ^{b} $R' = \{\Sigma[w(|F_o| - |F_c|)^2]/\Sigma[w|F_o|^2]\}^{\frac{1}{2}}$, $w = 1/\sigma(F_o)$.

Results and Discussion

Preparation.—Previously[9,10] the macrocycle $(L')^{2-}$ was prepared as $Cu^{II}Pb^{II}$ or $Ni^{II}Pb^{II}$ complexes by the reaction of [*N*,*N'*-bis(3-formyl-5-methylsalicylidene)ethane-1,2-diaminato]metal(II) (M = Cu or Ni) and diethylenetriamine in the presence of Pb^{2+} ion, and these complexes were used as precursors for a series of $Cu^{II}M^{II}$ and $Ni^{II}M^{II}$ complexes (M = Mn, Fe, Co, Ni, Cu or Zn). In this study a similar template reaction using 3-thiapentane-1,5-diamine instead of diethylenetriamine gave a mononuclear copper(II) complex containing a non-stoichiometric amount of perchloric acid, *i.e.* [CuL]·$n$$HClO_4$ (0 < n < 2). In this reaction Pb^{2+} ion is essential for forming the macrocycle, despite the lack of the ion in the product, because the non-template reaction between [*N*,*N'*-bis(3-formyl-5-methylsalicylidene)ethane-1,2-diaminato]copper(II) and 3-thiapentane-1,5-diamine gave a tarry material. The involvement of the non-stoichiometric amount of perchloric acid suggests the formation of two complexes in this reaction [CuL] and [Cu(H_2L)][ClO_4]$_2$. Thus, the reaction mixture was acidified to pH $\approx$ 3 with perchloric acid to obtain the diperchlorate salt [Cu(H_2L)][ClO_4]$_2$ **1**. The presence of the neutral form of the macrocycle (H_2L) in **1** is evidenced by complicated ν(O–H) vibrations in the region 3250–3100 cm^{-1}.

The reaction of complex **1** and a metal(II) perchlorate salt (M = Mn, Fe, Co, Ni or Zn) in methanol, in the presence of triethylamine as base, gave no precipitate of perchlorate complex but the addition of sodium thiocyanate to each reaction mixture resulted in the precipitation of the thiocyanate complexes [CuM(NCS)$_2$]·H_2O (M = Co **2**, Ni **3** or Zn **4**); the corresponding complexes with M = Mn or Fe were not precipitated. It should be mentioned that $(L')^{2-}$ forms $Cu^{II}M^{II}$

Table 2 Final atomic coordinates (× 10^4) with estimated standard deviations in parentheses for complex **4'**

Atom	x	y	z	Atom	x	y	z
Zn	1703(1)	3583(1)	4444(1)	C(14)	161(7)	4660(5)	3656(9)
Cu	775(1)	2119(1)	3477(1)	C(15)	−551(7)	4124(5)	3385(9)
S(1)	2401(2)	4641(2)	2405(3)	C(16)	−1440(7)	4405(6)	3094(10)
O(1)	1936(4)	2477(3)	4291(6)	C(17)	−2206(7)	3988(6)	2729(10)
O(2)	430(4)	3119(3)	3559(6)	C(18)	−3139(8)	4304(7)	2366(11)
N(1)	1027(6)	1129(4)	3962(8)	C(19)	−2063(7)	3255(6)	2699(9)
N(2)	3129(6)	3692(5)	4582(9)	C(20)	−1203(7)	2943(5)	2980(9)
N(3)	1029(6)	4562(4)	3979(7)	C(21)	−404(7)	3375(5)	3313(9)
N(4)	−462(6)	1784(4)	2985(8)	C(22)	−1188(7)	2163(6)	2829(11)
C(1)	1827(7)	892(5)	4423(10)	C(23)	−492(8)	1010(6)	2844(11)
C(2)	2648(7)	1317(5)	4674(9)	C(24)	207(8)	675(5)	3781(10)
C(3)	3469(8)	933(6)	5068(10)	S(2)	1174(3)	1338(2)	−270(3)
C(4)	4315(7)	1266(6)	5369(10)	N(5)	1157(6)	1961(6)	1826(9)
C(5)	5178(8)	854(6)	5812(11)	C(25)	1174(7)	1701(6)	963(10)
C(6)	4329(7)	1999(6)	5236(9)	S(3)	1048(4)	3647(3)	8088(4)
C(7)	3542(7)	2410(5)	4885(9)	N(6)	1592(7)	3584(5)	6076(8)
C(8)	2677(7)	2081(5)	4611(8)	C(26)	1356(9)	3616(7)	6922(10)
C(9)	3707(7)	3161(5)	4806(9)	O(3)	3805(12)	4092(7)	411(16)
C(10)	3567(7)	4402(6)	4576(10)	N(7)	3807(10)	2974(6)	1119(13)
C(11)	3524(8)	4628(6)	3344(11)	C(27)	4722(12)	3160(14)	1502(19)
C(12)	1860(8)	5391(6)	2959(10)	C(28)	3415(20)	2369(14)	1281(23)
C(13)	1553(7)	5248(5)	4034(9)	C(29)	3354(14)	3513(10)	529(18)

(M = Mn, Fe, Co, Ni or Zn) complexes as perchlorate salts.[9] On the other hand, the 1:1 reaction of **1** and copper(II) ion, in the presence of triethylamine, formed a perchlorate complex $[Cu_2L][ClO_4]_2$ **5** in good yield. Similarly, the reaction of **1** with Cu^I in the open air formed the $Cu^{II}Cu^I$ complex $[Cu_2L]ClO_4$ **6** in good yield. Apparently the N_2O_2S donor site of $(L)^{2-}$ has a high affinity for both Cu^{II} and Cu^I. It is also noteworthy that the copper(I) oxidation state is much stabilized in **6**, as judged from the stability towards molecular oxygen, probably due to donation from the thioether sulfur to the Cu^I.

Crystal Structure of $[CuZnL(NCS)_2]$·dmf **4'**.—An ORTEP[20] view of the complex is shown in Fig. 1 together with the numbering scheme. The relevant bond distances and angles are summarized in Table 3. The X-ray analysis clearly reveals a discrete CuZn dinuclear structure with the macrocycle $(L)^{2-}$ The Cu^{II} resides at the site with the CH_2CH_2 lateral chain and assumes a square-pyramidal geometry with N(1), N(4), O(1) and O(2) of L^{2-} at the basal plane and N(5) of a thiocyanate ion at the apex. The in-plane Cu–N and Cu–O bond distances fall in the range 1.921(7)–1.947(9) Å whereas the apical Cu–N(5) bond is significantly elongated [2.202(11) Å]. The Cu is 0.29 Å from the basal least-squares plane towards the apical N(5). The Zn^{II} resides at the site with the $CH_2CH_2SCH_2CH_2$ lateral chain and assumes a square-pyramidal geometry with N(2), N(3), O(1) and O(2) of $(L)^{2-}$ at the basal plane and N(6) of thiocyanate ion at the apex. The in-plane Zn–N and Zn–O bond distances fall in the range 2.102(8)–2.154(6) Å which are longer than the apical Zn–N(6) bond [2.003(10) Å]. The deviation of the Zn from the basal least-squares plane towards N(6) is 0.36 Å. The two isothiocyanato nitrogens, N(5) bound to Cu and N(6) bound to Zn, are *trans* to each other with respect to the macrocycle. The macrocycle forms a near coplane; the deviations of atoms, except for C(11), S(1) and C(12), from the least-squares plane are less than 0.43 Å. Atom S(1) is disposed towards the Zn^{II} but the Zn · · · S(1) interatomic separation (3.48 Å) is too large to be regarded as bonding. The X-ray structural result, however, indicates that the thioether sulfur may be involved in co-ordination to a metal ion with high affinity towards sulfur donors.

Physicochemical Properties.—All the complexes show two ν(C=N) vibrations at 1640–1630 cm^{-1}, in accord with the non-equivalent nature of the azomethine groups with respect to the two dissimilar lateral chains. Complexes **2** and **3** each show two ν(NC) modes of a thiocyanate group whereas the ν(NC) vibrations of **4** appear by chance as a superposed band. The ν(NS) mode for **2**–**4** is obscured but the δ(NCS) mode is clearly seen at ≈480 cm^{-1}. The frequency of the δ(NCS) mode implies co-ordination of the NCS^- ion through nitrogen,[21] in accord with the crystal structure of **4'**.

Based on molar conductance studies the thiocyanate complexes **2**–**4** behave as 1:1 electrolytes in dmf (see Experimental section). It is likely that the thiocyanate ion weakly bonded to the Cu^{II} is dissociated in dmf. The perchlorate complexes **5** and **6** behave as 2:1 and 1:1 electrolytes in dmf, respectively.

The electronic spectra of complexes **1**–**6** were obtained in dmf in the range 340–900 nm and the numerical data are given in Experimental section. All the complexes show an intense band in the near-ultraviolet region, assigned to the π–π* transition associated with the azomethine linkage.[22,23] The mononuclear complex **1** shows the azomethine π–π* band at 405 nm whereas for the dinuclear complexes **2**–**6** it occurs at shorter wavelengths (370–385 nm). Further, the absorption coefficient of the π–π* band of **2**–**6** (12 000–14 000 dm^3 mol^{-1} cm^{-1}) is significantly lower than that of **1** (20 500 dm^3 mol^{-1} cm^{-1}). Complex **1** shows a distinct visible band at 610 nm attributable to a superposed d–d band of Cu^{II}. This band shifts to shorter wavelengths for **2**–**6** (540–560 nm). In the case of **2** the d–d transition bands due to Co^{II} are concealed by the more intense copper(II) d–d band; a d–d component of Co^{II} is barely seen as a discernible shoulder near 600 nm. Similarly, **3** shows a discernible shoulder near 600 nm attributable to a d–d component of the Ni^{II}. The visible spectrum of **5** is characterized by another distinct band at 760 nm which is assigned to the Cu^{II} at the site with the $CH_2CH_2SCH_2CH_2$ lateral chain. A d–d band in the near-IR region means a distorted geometry about the Cu^{II}, effected by the co-ordination of the thioether sulfur. Such a near-IR band is not observed for the Cu^{II}_2 complex of $(L')^{2-}$.[9]

Complexes **1**, **4** and **6** have a magnetic moment characteristic for one unpaired electron (see Experimental section). On the other hand, **2**, **3** and **5** each shows a subnormal magnetic moment at room temperature, suggesting magnetic spin-exchange interaction within each molecule. The cryomagnetic properties of these complexes have been studied. Plots of $\chi_m T$ *vs.* T for **2** and **3** in the temperature range 4.2–290 K are available as SUP 57096. The plot of χ_m *vs.* T for **5** in the temperature range 80–290 K is shown in Fig. 2.

The $\chi_m T$ value of complex **2** (per CuCo) decreases with

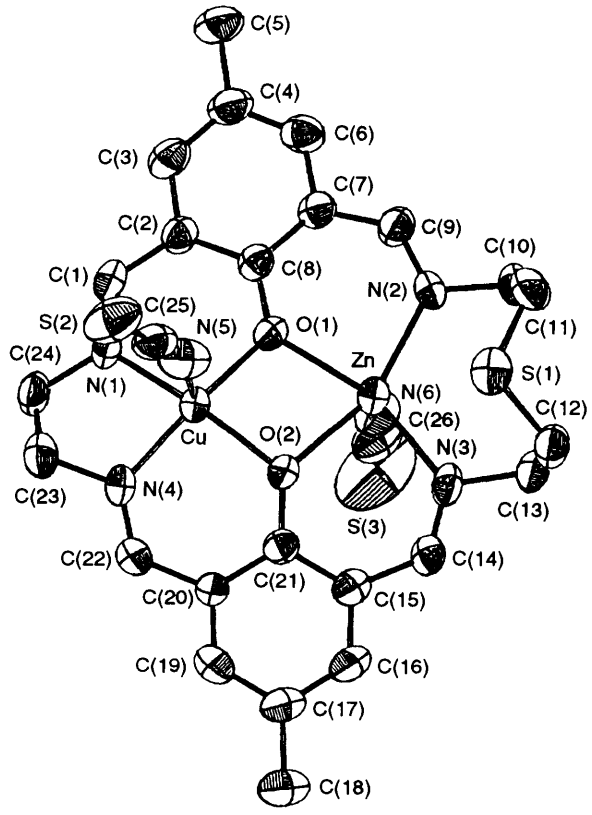

Fig. 1 An ORTEP view of $[CuZnL(NCS)_2]$·dmf **4'**

Table 3 Selected bond distances (Å) and angles (°) for **4'**

Cu–O(1)	1.921(7)	Zn–O(1)	2.105(7)
Cu–O(2)	1.942(7)	Zn–O(2)	2.154(6)
Cu–N(1)	1.947(9)	Zn–N(2)	2.118(9)
Cu–N(4)	1.924(10)	Zn–N(3)	2.102(8)
Cu–N(5)	2.202(11)	Zn–N(6)	2.003(10)
Cu · · · Zn	3.166(2)	Zn · · · S(1)	3.479(4)
Cu–O(1)–Zn	103.6(3)	Cu–O(2)–Zn	101.1(3)
O(1)–Cu–O(2)	82.1(3)	O(1)–Zn–O(2)	73.1(2)
O(2)–Cu–N(4)	94.5(3)	O(2)–Zn–N(3)	83.9(3)
N(4)–Cu–N(1)	84.0(4)	N(3)–Zn–N(2)	110.8(3)
N(1)–Cu–O(1)	94.7(3)	N(2)–Zn–O(1)	85.3(3)
N(5)–Cu–O(1)	96.9(3)	N(6)–Zn–O(1)	97.9(4)
N(5)–Cu–O(2)	107.4(4)	N(6)–Zn–O(2)	103.3(3)
N(5)–Cu–N(4)	95.8(4)	N(6)–Zn–N(2)	102.8(4)
N(5)–Cu–N(1)	94.1(4)	N(6)–Zn–N(3)	97.0(4)

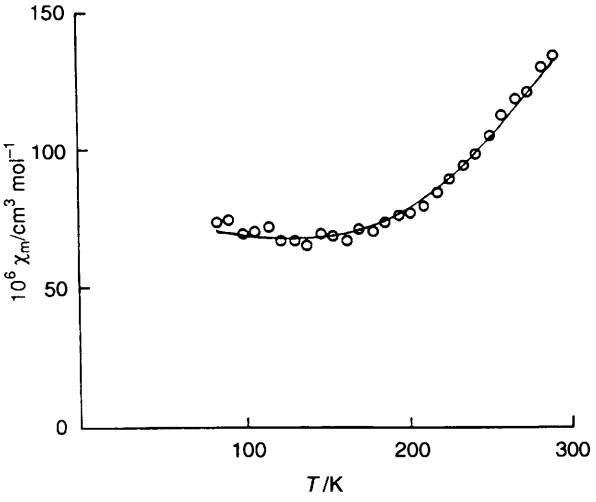

Fig. 2 Plot of χm *vs.* T for $[Cu_2L][ClO_4]_2$ **5**

decreasing temperature from 2.790 cm^3 mol^{-1} K (μ_{eff} = 4.72 μ_B) at 290 K to 0.442 cm^3 mol^{-1} K (1.88 μ_B) at 4.2 K. The moment at liquid-helium temperature is lower than the spin-only value for $S_T = 1$ resulting from spin coupling of Cu^{II} ($S = \frac{1}{2}$) and Co^{II} ($S = \frac{3}{2}$). This fact suggests that the antiferromagnetic interaction between the metal ions is dominant but some other effects contribute to the overall cryomagnetic property of this complex.

Magnetic analyses for $Cu^{II}Co^{II}$ complexes are not easy because of the orbital magnetic momentum of Co^{II}. In general, magnetic simulations have been made by taking into consideration the zero-field splitting of Co^{II} [24] or the Weiss parameter for interdimer interaction.[9] Our magnetic analyses for **2** are based on the Hamiltonian $H = -2JS_1S_2 - DS_z^2$ and the magnetic susceptibility expression in this case has been derived by Lambert *et al.*[24] The cryomagnetic behaviour of **2** could be tolerably reproduced by this expression, using $J = -32$ cm^{-1}, $g = 2.37$, $D = -4.60$ cm^{-1} and $N\alpha = 380 \times 10^{-6}$ cm^3 mol^{-1}. The discrepancy factor defined as $R(\chi) = [\Sigma(\chi_{obs} - \chi_{calc})^2/\Sigma(\chi_{obs})^2]^{\frac{1}{2}}$ was 0.16.

The $\chi_m T$ value of complex **3** (per CuNi) at 290 K is 1.136 cm^3 mol^{-1} K (μ_{eff} = 3.01 μ_B) which decreases with decreasing temperature to a minimum of 0.398 cm^3 mol^{-1} K (1.78 μ_B) near 34 K, increases to a maximum of 0.464 cm^3 mol^{-1} K (1.93 μ_B) near 10 K, and then decreases again below 10 K. The magnetic behaviour at low temperature suggests a secondary magnetic contribution in addition to the dominant antiferromagnetic spin exchange between the Cu^{II} and Ni^{II}. The drop in $\chi_A T$ value below 10 K may be ascribed to the zero-field splitting of Ni^{II} (ref. 25) or interdimer antiferromagnetic interaction, but the magnetic behaviour in the range 10–30 K is unusual. Thus, we first attempted to simulate magnetization in the temperature range 30–300 K, by means of the magnetic susceptibility equation for ($S_1 = \frac{1}{2}$)–($S_2 = 1$) based on the isotropic Heisenberg model (1) where $g_{\frac{1}{2}}$ and $g_{\frac{3}{2}}$ are g factors associated

$$\chi_m = [N\beta^2/4k(T - \theta)][10g_{\frac{1}{2}}^2 + g_{\frac{3}{2}}^2 \exp(-3J/kT)]/[2 + \exp(-3J/kT)] \quad (1)$$

with the $S_T = \frac{1}{2}$ and $\frac{3}{2}$ states, respectively, and derived arithmetically[26,27] using local g factors for Ni^{II} and Cu^{II} as $g_{\frac{1}{2}} = (4g_{Ni} - g_{Cu})/3$ and $g_{\frac{3}{2}} = (2g_{Ni} + g_{Cu})/3$. The simulation with equation (1), however, gave very poor fitting especially in the low-temperature region. Eventually we found that a better magnetic simulation is obtained over the temperature range 7–300 K, except at 10–90 K, using $J = -90$ cm^{-1}, $g_{Cu} = 2.10$, $g_{Ni} = 2.18$, $\theta = -0.2$ K and $N\alpha = 280 \times 10^{-6}$ cm^3 mol^{-1}. The discrepancy factor in this simulation was 7.88×10^{-2}. It appears that the decreased magnetization in the temperature range 10–90 K is due to a phase transition like 'reentrant' behaviour.[28]

The magnetic susceptibility χ_A of complex **5** (per Cu) decreases with decreasing temperature from 134×10^{-6} cm^3 mol^{-1} at 290 K to a round minimum of 65×10^{-6} cm^3 mol^{-1} around 120 K (see Fig. 2). The minimum corresponds to the temperature-independent paramagnetism of Cu^{II} arising from the second-order Zeeman effect. The result indicates a very strong antiferromagnetic spin coupling between a pair of copper(II) ions. A slight increase in magnetic susceptibility is seen below 120 K which probably arises from contamination by a small amount of paramagnetic impurity. Thus, the magnetic simulation for **5** was performed by the use of Bleaney–Bowers equation [29] (2) including a correction term for the paramagnetic

$$\chi_A = (Ng^2\beta^2/kT)[3 + \exp(-2J/kT)]^{-1}(1 - \rho) + (0.45\rho/T) + N\alpha \quad (2)$$

impurity. In this equation ρ is the fraction of paramagnetic impurity. A good magnetic simulation has been obtained by this equation as shown by the trace in Fig. 2, using $J = -440$ cm^{-1}, $g = 2.10$, $N\alpha = 60 \times 10^{-6}$ cm^3 mol^{-1} and $\rho = 0.002$. The discrepancy factor was 2.57×10^{-2}.

Complex **5** shows very strong antiferromagnetic interaction relative to the dinuclear copper(II) complex of $(L')^{2-}$, $[Cu_2L'][ClO_4]_2$ ($J = -62$ cm^{-1}). This is probably related to the different core structures of the complexes which remain to be elucidated by X-ray structural studies.

The solution ESR spectra of complexes **1**, **4** and **6** are typical of planar or axially distorted Cu^{II}, showing $g_{av} \approx 2.1$ and $A_{av} \approx 8.6 \times 10^{-3}$ cm^{-1} at room temperature and $g_{\|} \approx 2.10$, $g_{\perp} \approx 2.05$ and $A_{\|} = 2.0 \times 10^{-2}$ cm^{-1} at liquid-nitrogen temperature. Thus, the spin is localized in the mixed-valence complex **6**, *i.e.* Class 1 according to the classification of Robin and Day.[30]

Complex **2** showed no ESR signal at liquid-nitrogen temperature, probably owing to the magnetic interaction between the Cu^{II} and Co^{II}. Similarly, **5** is ESR silent because of the strong antiferromagnetic interaction between the two copper(II) ions.

There are few ESR spectroscopic studies on magnetically interacting Cu^{II} and Ni^{II} systems [24,25,31] in spite of considerable studies by bulk magnetic susceptibility measurements. Complex **3** showed fairly well resolved ESR signals when measured as a frozen dmf solution at liquid-nitrogen temperature. The spectrum is regarded as an axial pattern with $g_{\|} \approx 2.1$ and $g_{\perp} \approx 2.2$ despite very poor resolution of the $g_{\|}$ component (see SUP 57096). A similar ESR spectrum has been reported previously for a related macrocyclic $Cu^{II}Ni^{II}$ complex.[24] It should be mentioned that the order $g_{\perp} > g_{\|}$ corresponds to an axially distorted d^9 configuration with one unpaired electron in the d_{z^2} orbital.[32]

The energy separation between the spin-singlet ground state and spin-quartet excited state for a $Cu^{II}Ni^{II}$ complex ($S_{Ni} = 1$) is given by $-3J$ which corresponds to 246 cm^{-1} for **3**. This means that the thermal population of the spin-quartet excited state is negligibly small at liquid-nitrogen temperature and the ESR signals observed for **3** arise from the spin-doublet ground state. In general spin coupling through $d_{x^2-y^2}$(Cu)–$d_{x^2-y^2}$(Ni) in a $Cu^{II}Ni^{II}$ complex is strongly antiferromagnetic as demonstrated for many dinuclear copper(II) complexes [33,34] as well as for **5**, one unpaired electron remaining in the d_{z^2}(Ni) orbital (local x and y axes are taken as along the donor atoms in the equatorial plane). The observed spectral feature $g_{\perp} > g_{\|}$ is in accord with this, but the broad $g_{\|}$ feature, probably due to the copper nucleus,[24] suggests the delocalization of one unpaired electron over the CuNi core.

The electrochemical properties of complexes **2**–**6** were studied by means of cyclic voltammetry. The cyclic voltammograms of **2**–**4** showed complicated waves which

varied upon changing the sweep range and also upon repetition of the sweep. Thus, assignments of the waves could not be made, except for the anodic wave near +0.8 V (*vs.* SCE) attributable to the oxidation of NCS^- ion. In this study our attention was focused on the electrochemical behaviour of **5** ($Cu^{II}Cu^{II}$) and **6** ($Cu^{II}Cu^{I}$).

The cyclic voltammogram of complex **5** shows a reversible couple at +0.07 V (*vs.* SCE) and a quasi-reversible couple at −1.02 V. They are assigned to the stepwise reduction processes $Cu^{II}Cu^{II} \longrightarrow Cu^{II}Cu^{I}$ and $Cu^{II}Cu^{I} \longrightarrow Cu^{I}Cu^{I}$ respectively.[9] Essentially the same cyclic voltammogram was obtained for **6** (+0.09 and −1.01 V). The $Cu^{II}{}_2$ complex of $(L')^{2-}$ shows corresponding reduction waves at −0.35 and −1.09 V in dimethyl sulfoxide. In spite of the different solvents in the electrochemical mesurements, **5** shows the first reduction (of the Cu^{II} at the N_2O_2S donor site) at a significantly higher potential. The positive shift of the reduction potential and the good reversibility of the first wave are indicative of the stabilization of the copper(I) oxidation state at the N_2O_2S site, effected by the co-ordination of thioether sulfur.[35] The cyclic voltammogram of **5** is available as SUP 57096.

From the above discussion it is seen that the macrocycle $(L)^{2-}$ is a promising dinucleating ligand for complexes with $M^{II}Cu^{I}$ cores

References

1 P. A. Vigato, S. Tamburini and D. E. Fenton, *Coord. Chem. Rev.*, 1990, **106**, 25.
2 S. Gambarotta, F. Arena, C. Floriani and P. F. Zanazzi, *J. Am. Chem. Soc.*, 1982, **104**, 5082; F. Arena, C. Floriani, A. Chiesi-Villa and C. Guastini, *Inorg. Chem.*, 1986, **25**, 4589.
3 M. Sakamoto, M. Takagi, T. Ishimori and H. Ōkawa, *Bull. Chem. Soc. Jpn.*, 1988, **61**, 1613; M. Sakamoto, T. Ishimori and H. Ōkawa, *Bull. Chem. Soc. Jpn.*, 1988, **61**, 3319; Y. Aratake, H. Ōkawa, E. Asato, H. Sakiyama, M. Kodera, S. Kida and M. Sakamoto, *J. Chem. Soc., Dalton Trans.*, 1990, 2941.
4 O. Kahn, *Struct. Bonding (Berlin)*, 1987, **68**, 89.
5 E. Sinn and C. M. Harris, *Coord. Chem. Rev.*, 1969, **4**, 391.
6 U. Casellato, P. A. Vigato and M. Vidali, *Coord. Chem. Rev.*, 1977, **23**, 31; P. Zanello, S. Tamburini, P. A. Vigato and G. A. Mazzocchin, *Coord. Chem. Rev.* 1987, **77**, 165.
7 J. J. Christensen and D. J. Eatough, *Coordination Chemistry of Macrocyclic Compounds*, ed. G. A. Melson, Plenum, New York, 1979, p. 145.
8 J. F. Endicott and B. Durham, *Coordination Chemistry of Macrocyclic Compounds*, ed. G. A. Melson, Plenum, New York, 1979, p. 393.
9 H. Ōkawa, J. Nishio, M. Ohba, M. Tadokoro, N. Matsumoto, M. Koikawa, S. Kida and D. E. Fenton, *Inorg. Chem.*, 1993, **32**, 2949.
10 J. Nishio, H. Ōkawa, S. Ohtsuka and M. Tomono, *Inorg. Chim. Acta*, 1994, **218**, 27.
11 E. J. Larson and V. L. Pecoraro, *J. Am. Chem. Soc.*, 1991, **113**, 3810; T. Matsushita, T. Yarino, I. Masuda, T. Shono and K. Shinra, *Bull. Chem. Soc. Jpn.*, 1973, **46**, 1712; T. Yarino, T. Matsushita, I. Masuda and K. Shinra, *Chem. Commun.*, 1970, 1317.
12 R. D. Jones, D. A. Summerville and F. Basolo, *Chem. Rev.*, 1979, **79**, 139; E. Ochiai, *J. Inorg. Nucl. Chem.*, 1973, **35**, 1727; G. McLendon and A. E. Martell, *Coord. Chem. Rev.*, 1976, **19**, 1.
13 C. Floriani and F. Calderazzo, *Coord. Chem. Rev.*, 1972, **8**, 57.
14 N. F. Curtis, *J. Chem. Soc.*, 1961, 3147.
15 L. N. Mulay, *Theory and Applications of Molecular Paramagnetism*, eds. E. A. Boudreaux and L. N. Mulay, Wiley, New York, 1976, p. 491.
16 H. Ōkawa and S. Kida, *Bull. Chem. Soc. Jpn.*, 1972, **45**, 1759.
17 D. A. Denton and H. Suschitzky, *J. Chem. Soc.*, 1963, 4741.
18 A. E. Martin and J. E. Bulkowski, *J. Org. Chem*, 1982, **47**, 415.
19 *International Tables for X-Ray Crystallography*, eds. J. A. Ibers and W. C. Hamilton, Kynoch Press, Birmingham, 1974, vol. 4.
20 C. K. Johnson, ORTEP, Report ORNL-5138, Oak Ridge National Laboratory, Oak Ridge, TN, 1976.
21 A. Sabatini and I. Bertini, *Inorg. Chem.*, 1965, **4**, 959.
22 B. Bosnich, *J. Am. Chem. Soc.*, 1968, **90**, 627.
23 R. S. Downing and F. L. Urbach, *J. Am. Chem. Soc.*, 1969, **91**, 5977.
24 S. L. Lambert, C. L. Spiro, R. R. Gagne and D. N. Hendrickson, *Inorg. Chem.*, 1982, **21**, 68.
25 Y. Journaux, O. Kahn, I. Morgenstern-Badarau, J. Galy, J. Jaud, A. Bencini and D. Gatteschi, *J. Am. Chem. Soc.*, 1985, **107**, 6305.
26 C. C. Chao, *J. Magn. Reson.*, 1973, **10**, 1.
27 R. P. Scaringe, D. J. Hodgson and W. E. Hatfield, *Mol. Phys.*, 1978, **35**, 701.
28 K. Agawa, T. Okuno, Y. Maruyama, A. Kobayashi, H. Kobayashi, S. Schenk and A. E. Underhill, *Inorg. Chem.*, 1994, **33**, 5598.
29 B. Bleaney and K. D. Bowers, *Proc. R. Soc. London, Ser. A*, 1952, **214**, 451.
30 M. B. Robin and P. Day, *Adv. Inorg. Chem. Radiochem.*, 1967, **10**, 247.
31 I. Morgenstern-Badarau, M. Rerat, O. Kahn, J. Jaud and J. Galy, *Inorg. Chem.*, 1982, **21**, 3050.
32 B. A. Goodman and J. B. Raynor, *Adv. Inorg. Chem. Radiochem.*, 1970, **13**, 135.
33 M. Melnik, *Coord. Chem. Rev.*, 1982, **42**, 259.
34 C. J. Cairns and D. H. Busch, *Coord. Chem. Rev.*, 1986, **69**, 1.
35 M. Mikuriya, M. Nakamura, H. Ōkawa and S. Kida, *Chem. Lett.*, 1982, 839.

Received 1*st March* 1995; *Paper* 5/01257K